Synthesis of Rh–carbon nanotube based heterostructures and their enhanced field emission characteristics†

Bhaskar R. Sathe, Bhalchandra A. Kakade, Ajay Kushwaha, Mohammed Aslam and Vijayamohanan K. Pillai*

Received 22nd May 2010, Accepted 25th June 2010
DOI: 10.1039/c0cc01532f

Selective decoration of Rh nanospheres on acid functionalized carbon nanotubes has been demonstrated using Al as a sacrificial substrate. Remarkable field emission has been observed for this heterostructure as a high current density of 170 μA cm^{-2} is generated at an ultra-low threshold of 300 V μm^{-1}, compared to much smaller values for Rh nanospheres and carbon nanotubes separately.

Metal nanostructures of tunable size and shape have been the central focus of current research due to their unusual electronic, optical and magnetic properties that are often different from those of their bulk counterparts.[1] The exploitation of the electronic structure of these materials at the nanoscale has strong implications for the development of high-throughput electronic devices, like those based on field emission.[2] Field emission from nanostructured materials, in particular, has captured extensive attention in the past few years due to the enormous field enhancement possible at sharp tips anticipated as a function of their size and shape in the nanoscale.[3] Moreover, carbon-based materials such as diamond, carbon nanotubes (CNTs), graphenes *etc*. are more favorable in terms of their stability and mechanical strength.[4] Unfortunately, their higher resistivity diminishes their replenishment and transport of electrons, thereby requiring higher threshold fields with time to sustain a constant emission current.[5] Since carbon nanotubes are already considered to be good emitters,[6] their desirable properties may be further enhanced by making use of the electronic properties (work function and the structure of density of states) of metal decorated CNT heterostructures since some of these can operate remarkably well (lower applied voltages) below the intrinsic current limit due to their thermal effects.[7]

Current strategies of binding nanoparticles to carbon nanotubes (CNTs) often make use of small organic bridging molecules to improve the adhesion between the nanostructures and CNTs.[8] This not only complicates the process but also results in indirect and poorer contact between different phases. Indeed, the consequential increase in the barrier for electron transport can adversely affect materials performance in emission applications.[9] Enormous improvements have been made, to date, in metal/CNT heterostructures using silver (Ag), platinum (Pt), nickel (Ni), palladium (Pd), rhodium (Rh) and gold (Au) despite the poor durability issues for some of these heterostructures.[8,10] Among these, Rh/CNTs could especially be promising due to their features such as excellent electrical performance, chemical inertness, mechanical strength, remarkable thermal stability, lower electron affinity and significant stability toward ion bombardment.[11]

Herein we report such an enhanced field emission from Rh nanospheres decorated multiwalled carbon nanotubes (MWNTs) as compared to Rh nanospheres and acid functionalized MWNTs. Raman spectroscopic analysis reveals conclusive mechanistic evidence for oxidative functionalization followed by effective decoration of Rh nanospheres at the defect sites of the carbon nanotubes as a primary reason for the enhanced emission. An ultra-low threshold field of 300 V μm^{-1} has been observed to generate a comparatively high field emission current density of 170 μA cm^{-2} for Rh nanospheres decorated MWNTs while Rh nanospheres and acid functionalized MWNTs display 54 μA cm^{-2} and 32 μA cm^{-2} respectively under similar experimental conditions. Higher current density at this ultra-low threshold field indicates that the origin of the extraordinary electron emission performance is from the co-operative interactions between Rh nanospheres and MWNTs. More significantly, further tuning of the size and distribution could offer several promising characteristics specially required for the development of high performance electron sources.

Synthesis of these Rh/MWNTs heterostructures briefly involves electroless reduction of Rh ions in the presence of acid functionalized MWNTs using Al as a reducing substrate. The synthetic strategy is briefly (schematically) shown in Scheme 1, although more details of the steps involved in the formation of Rh/MWNTs heterostructures, Rh nanospheres synthesis and functionalization of MWNTs are presented in the experimental section.†

Fig. 1(a) shows a typical scanning electron microscopy (SEM) image of Rh nanospheres decorated on the surface of acid functionalized MWNTs having uniform and monodispersed

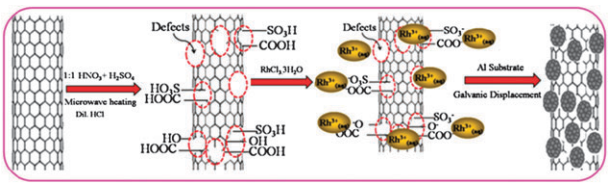

Scheme 1 Schematic representation of assembling procedure for the decoration of Rh nanospheres on acid functionalized multiwalled carbon nanotubes.

Physical and Materials Chemistry Division, National Chemical Laboratory, Pune 411008, India. E-mail: vk.pillai@ncl.res.in; Fax: +91-20-25882636; Tel: +91-20-25882636
† Electronic supplementary information (ESI) available: Experimental details, SEM and TEM images of Rh nanospheres and MWNTs. See DOI: 10.1039/c0cc01532f

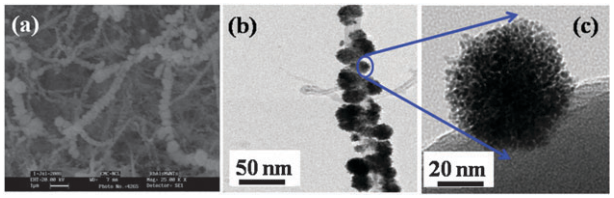

Fig. 1 (a) SEM image of as-prepared Rh-MWNTs using galvanic displacement approach. (b) TEM of single Rh-MWNTs. (c) High resolution TEM image of single Rh nanospheres on MWNTs surface, showing aggregation of small nanoparticles with average diameter of 2.3 nm.

coverage. Accordingly, a high density of Rh nanoparticles (~2.3 nm size) coalesced into assembled nanospheres having a size of 150 nm with a monodispersed decoration throughout the MWNTs wall can be clearly seen in the transmission electron microscopic images of Fig. 1(b and c).

The reduction of Rh atoms on the defect sites/oxidized sites of the MWNTs instead of that within the solution and on the surface of the Al substrate could be due to the initial replacement of H^+ of the acidic functionalities of nanotubes with Rh^{3+} ions. Further, the Al substrate supports these Rh ions to undergo reduction on this already well-stabilized carbon nanotube platform so that these nanoparticles having extremely high surface energy are formed through spherical growth (see Fig. 1). These spheres and their direct interactions with MWNTs walls are revealed by the high resolution transmission electron microscopic image as revealed in Fig. 1(c) and Scheme 1 respectively. This hetero-structure assembly is believed to be responsible for their enhanced field emission, despite their having higher size due to assembly of small particles. The unique morphological features (when compared to other regular spheres) include their central thicker core and rougher, comparatively less dense outer surface region having a diameter of ~150 nm. Similar Rh nanospheres synthesized using an identical procedure but without carbon nanotubes clearly indicate these nanospheres have irregular surface morphology, despite having the same average diameter of ~150 nm (SI-I†). However, the spacing is the same for assembled nanoparticles (~2.3 nm) after an internal assembly to nanospheres with a good monodispersion as has been clearly seen in TEM images (SI-I†). Furthermore, SEM and TEM images of acid functionalized MWNTs confirm an average thickness of ~30 nm (SI-II†).

Raman spectroscopy has also been employed to strengthen our interpretation of efficient acid functionalization followed by decoration of Rh nanospheres on the surface of MWNTs. Accordingly, Fig. 2a presents a comparison of the Raman spectra of the pristine, acid treated and Rh nanospheres decorated MWNTs each of them consisting of two characteristic bands. The band at 1320 cm^{-1} (for pristine), 1327 cm^{-1} (for oxidized) and 1332 cm^{-1} (for Rh nanospheres decorated MWNTs) is the D band, which is caused by the induction of significant defects or disorder in the CNT surfaces.[12] The G band corresponding to the crystallite graphitic structure is obtained at 1578 cm^{-1} (pristine), 1581 cm^{-1} (oxidized) and 1583 cm^{-1} (Rh nanospheres decorated MWNTs).

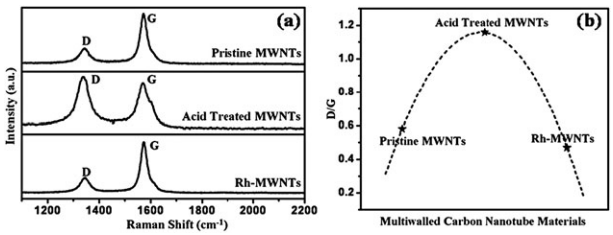

Fig. 2 (a) Raman spectra of the pristine, acid treated and Rh nanospheres decorated MWNTs. (b) The change in intensity ratio of D to G band of MWNTs with oxidation and the subsequent decoration with Rh nanospheres.

The D and G peaks have been analyzed for the intensity ratio (D/G) to quantify the surface oxidation process along with their concomitant topographic effects. Accordingly, Fig. 2b shows the D/G values for the pristine, acid functionalized and Rh nanospheres decorated carbon nanotubes. The surface oxidized carbon nanotubes have a higher D/G ratio than that for the pristine carbon nanotubes, which is indicative of oxidative functionalization although a further oxidation process causes a continuous increase in the number of defective sites, which presumably increases the reactivity of the MWNTs.[13]

The distribution of defect sites on the nanotube lattice is due to breaking of some of the walls of the MWNTs by oxidation (Scheme 1). These defects include the conversion of sp^2-hybridized carbon to sp^3-hybridized carbon during the oxidation process, with the creation of carboxylic and hydroxyl groups. In particular, the D/G ratio decreases significantly after formation of the heterostructures. This suggests that the defect sites generated on the MWNTs surface during oxidation can be passivated by the Rh nanospheres decoration (Fig. 1 and 2) along with their red shifting of both D and G bands. The increase in D/G ratio (Fig. 2b) together with shifting of G and D bands (Fig. 2a) seems to be related to the strong bond between surface oxidized carbon (carbon defects) and surface Rh-atoms of nanospheres.

Having demonstrated the unique morphological features of these nanostructured Rh/MWNTs we investigated the co-operative effects between Rh nanospheres and MWNTs as compared to that of "as-synthesized" Rh nanostructures by

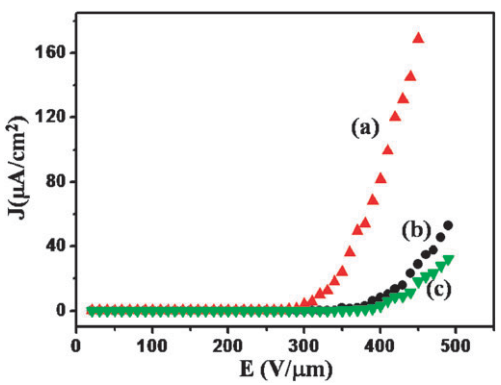

Fig. 3 Field emission (*J*–*E*) characteristics for (a) Rh-MWNTs, (b) Rh nanospheres and (c) acid functionalized MWNTs mounted on Si, revealing typical metallic behavior.

Table 1 Comparison of the field-emission performance of our heterostructures with some recently reported nanostructures

Sr. No.	Emitter Nanostructures	Synthesis method	Turn-on field	Field-enhancement factor (β)	Reference
1	Rh/MWNTs	Galvanic Displacement with Al	168 μA cm^{-2} at 450 V μm^{-1}	9820	Present work
2	Rh nanospheres	Galvanic Displacement with Al	54 μA cm^{-2} at 490 V μm^{-1}	1880	Present work
3	Acid functionalized MWNTs	Chemical Vapor Deposition	32 μA cm^{-2} at 490 V μm^{-1}	1070	Present work
4	Rh Hexagons	Chemical Vapor Deposition	4×10^{-3} μA cm^{-2} at 0.72 V μm^{-1}	9325	3
5	Er/MWNTs	Chemical Vapor Deposition	3.4 mA cm^{-2} at 1.8 V μm^{-1}	2543	14
6	SiC/Si Heterostructures	High temperature carbon implantation into Si	2.6 V μm^{-1} at 1 μA cm^{-2}	—	15

the same approach and also that of acid functionalized MWNTs towards their emission performance. Accordingly, Fig. 3 shows typical superimposed emission current density *vs.* applied electric field curves for the diode configuration of (a) Rh nanospheres decorated carbon nanotubes, (b) Rh nanospheres and (c) acid functionalized MWNTs respectively.

Both the turn-on field and the higher current density of the Rh/MWNTs indicate that the field emission from the Rh nanospheres decorated on MWNTs is enhanced considerably, where an onset field of 260 V μm^{-1}, requiring an emission current of 6.5 nA (corresponding to the current density of 2.5×10^{-3} μA cm^{-2}), is reproducibly observed. The emission current density of the Rh decorated MWNTs measured at 450 V μm^{-1} improves from 32 μA cm^{-2} (acid functionalized MWNTs) to 54 μA cm^{-2} (Rh nanospheres) to 68 μA cm^{-2}. In addition, turn-on field decreases from 340 V μm^{-1} (acid treated MWNTs) to 270 V μm^{-1} (Rh/MWNTs) (shown in Table 1), which could be due to the co-operative effects.

The enhanced emission properties can be explained on the basis of reduced turn-on field and improvement in emission current density related to the Rh nanospheres anchored on CNTs. The functionalization of CNT using Rh nanoclusters presumably decreases the local work function of the field emitters enabling an increase in the density of states (DOS) near the Fermi level of the CNTs surface due to the co-operative nature of the electronic interactions with Rh. However, only moderate field emission is observed from acid functionalized MWNTs as compared to that of the other two emitters (Rh decorated MWNTs and Rh nanospheres). This may be due to the fact that many defect sites created by the acid treatment contain many oxygen functional groups along with the destruction of regular graphitic structure on the surface, which automatically reduces the emission current/site density. Accordingly, comparison of the field-emission performance of our emitter materials along with a list of some recently reported nanostructures is shown in Table 1.

In summary, a unique Rh–carbon nanotube based heterostructure has been demonstrated by the controlled decoration of Rh nanospheres (2.3 nm) on acid functionalized MWNTs surface ($\sim$150 nm) enabling enhanced field emission behavior. The synthesis consists of acid functionalization of MWNTs followed by further simple ion exchange, for replacing the proton of acid functionalities by Rh^{3+} ions and subsequent reduction of these ions by a galvanic approach. An ultra-low threshold field of 300 V μm^{-1} is observed to generate an emission current density of 170 μA cm^{-2}, which is appreciably larger as compared to that of individual Rh nanospheres (54 μA cm^{-2}) and functionalized MWNTs (32 μA cm^{-2}). This process can easily be scaled up using larger Al substrates and by tuning the extent of functionalization on MWNTs which would be useful in microelectronics and also for field emission displays. The smaller size of emitting area along with the possibility of modulating their co-operative interaction promises remarkable characteristics for development of futuristic field emission devices.

Notes and references

1 A. M. Smith, A. M. Mohs and S. Nie, *Nat. Nanotechnol.*, 2009, **4**, 56.
2 M. E. Stewart, C. R. Anderton, L. B. Thompson, J. Maria, S. K. Gray, J. A. Rogers and R. G. Nuzzo, *Chem. Rev.*, 2008, **108**, 494.
3 R. B. Sharma, D. J. Late, D. S. Joag, A. Govindaraj and C. N. R. Rao, *Chem. Phys. Lett.*, 2006, **428**, 102; B. R. Sathe, B. A. Kakade, I. S. Mulla, V. K. Pillai, D. J. Late, M. A. More and D. S. Joag, *Appl. Phys. Lett.*, 2008, **92**, 253106.
4 S. Iijima, *Nature*, 1991, **354**, 56; G. G. Wildgoose, C. E. Banks and R. G. Compton, *Small*, 2006, **2**, 182; Y. Lin, S. Taylor, H. Li, K. A. Shiral Fernando, L. Qu, W. Wang, L. Gu, B. Zhou and Y. P. Sun, *J. Mater. Chem.*, 2004, **14**, 527.
5 T. C. Choy, A. M. Stoneham and A. H. Harker, *J. Phys.: Condens. Matter*, 2005, **17**, 1505.
6 N. De Jonge, Y. Lamy, K. Schoots and T. Oosterkamp, *Nature*, 2002, **420**, 393; W. A. de Heer, A. Chatelain and D. Ugarte, *Science*, 1995, **270**, 1179.
7 R. B. Rakhi, A. L. Reddy, M. M. Shaijumon, K. Sethupathi and S. Ramaprabhu, *J. Nanopart. Res.*, 2008, **10**, 179; A. Liu, K. S. Kim, J. Baek, Y. Cho, S. Han and S. W. Kim, *Carbon*, 2009, **47**, 1158; T. Jeong, J. Heo, J. Lee, S. Lee, W. Kim, H. Lee, S. Park, J. M. Kim, T. Oh, C. Park, J. Yoo, B. Gong, N. Lee and S. G. Yu, *Appl. Phys. Lett.*, 2005, **87**, 063112.
8 B. A. Kakade, S. Sahoo, S. B. Halligudi and V. K. Pillai, *J. Phys. Chem. C*, 2008, **112**, 13317.
9 B. Akdim, S. N. Kim, R. R. Naik, B. Maruyama, M. J. Pender and R. Pachter, *Nanotechnology*, 2009, **20**, 355705.
10 B. Yoon and C. Wai, *J. Am. Chem. Soc.*, 2005, **127**, 17174; A. Klinke, E. Delvigne, J. V. Barth and K. Kern, *J. Phys. Chem. B*, 2005, **109**, 21677; Y. Fan, M. Burghard and K. Kern, *Adv. Mater.*, 2002, **14**, 130.
11 A. A. Cotton and G. Wilkinson, *Advanced Inorganic Chemistry*, Wiley, New York, 7th edn, 2007; S. W. Rosencrance, J. S. Burnham, D. E. Sanders, C. He, B. J. Garrison, N. Winograd, Z. Postawa and A. E. De Pristo, *Phys. Rev. B: Condens. Matter*, 1995, **52**, 6006.
12 K. A. Worsley, I. Kalinina, E. Bekyarova and R. C. Haddon, *J. Am. Chem. Soc.*, 2009, **131**, 18153.
13 K. T. Nguyen and M. Shim, *J. Am. Chem. Soc.*, 2009, **131**, 7103; S. Y. Lee, W. C. Choi, C. Jeon, C. Park, J. H. Yang and M. H. Kwon, *Appl. Phys. Lett.*, 2008, **93**, 103101.
14 S. Shrestha, W. C. Choi, W. Song, Y. T. Kwon, S. P. Shrestha and C. Park, *Carbon*, 2010, **48**, 54.
15 X. Fang, Y. Bando, U. Gautam, C. Ye and D. Golberg, *J. Mater. Chem.*, 2008, **18**, 509.